

11.11 **GUINEA GULF SST AND MEDITERRANEAN SUMMER CLIMATE:  
ANALYSIS OF THE INTERANNUAL VARIABILITY**

**Marina Baldi\***, Francesco Meneguzzo, Giovanni A. Dalu, Giampiero Maracchi,  
Massimiliano Pasqui, Valerio Capecchi, Alfonso Crisci, Francesco Piani

Institute of Biometeorology – National Research Council (CNR-IBIMET), Via Caproni 8,  
50145 - Firenze, Italy.

## 1. ABSTRACT

During the boreal summer, fluctuations of the West Africa monsoon are known to produce significant changes of the regional atmospheric circulation which affects rainfall, moisture, temperature and wind, as far north as the central Sahara desert.

Latitudinal shifts of the monsoon are partly connected to the anomalous warming of the sea surface in the Guinea Gulf near the equator, providing a connection between the Guinean coastal region and the Sahel through feedback between the thermodynamics forcing and the dynamics. Warm SSTAs in the Gulf of Guinea bring more rain near the coast, while cold SSTAs are favourable to a deeper inland development of the West Africa monsoon (Figure 1).

An interannual climatological analysis suggests that the SSTs (mean and anomalies) in the Guinea Gulf, through their effect on the West Africa monsoon, influence the central-western Mediterranean summer (see Figure 2, 3), and,

affecting the temperature and precipitation, give rise to an anomalous summertime climate.

A southward shift of the monsoon is related to cooler and wetter conditions over the central and western Mediterranean sea in mid-late summer. While, when the monsoon influence moves further North, the summer becomes hot and dryer in the western the Mediterranean region.

Statistical analysis of climatological data over the region, and of NCEP/NCAR reanalysis and regional numerical simulations show the effectiveness of the SST and SST Anomalies in the Gulf of Guinea in modifying the Mediterranean summer climate.

## 2. INTRODUCTION

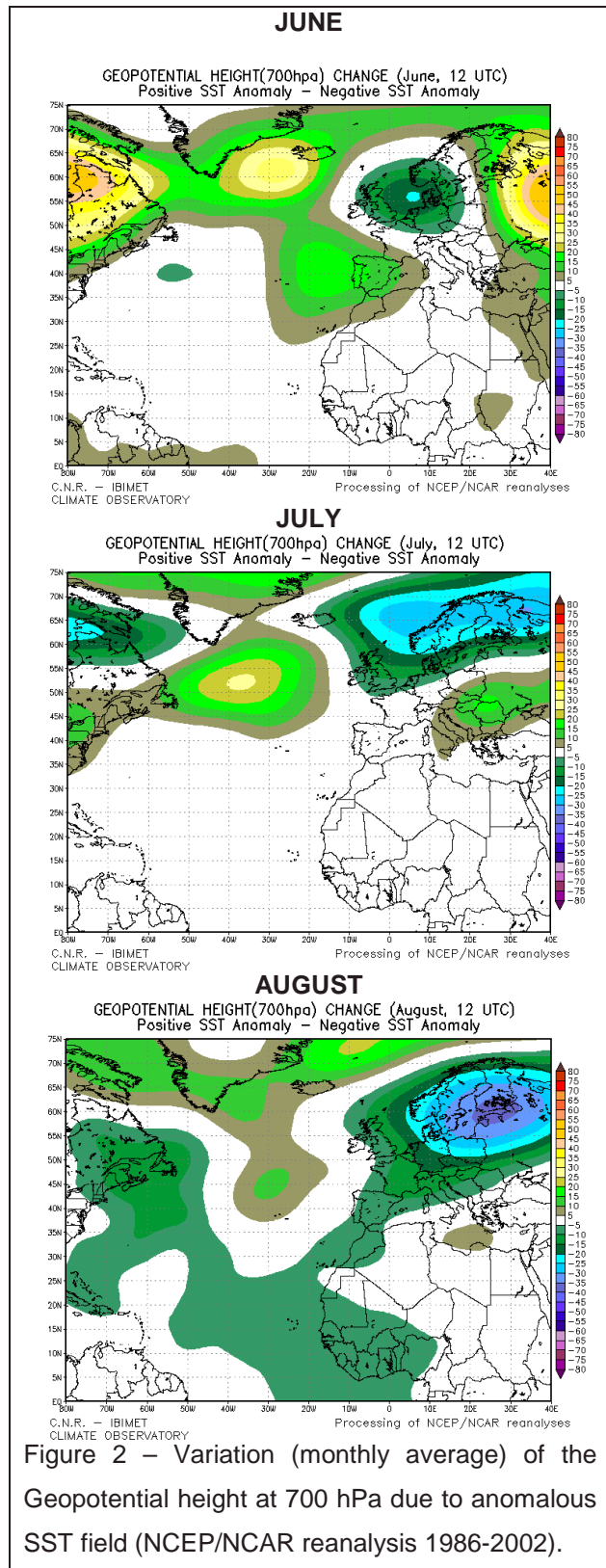
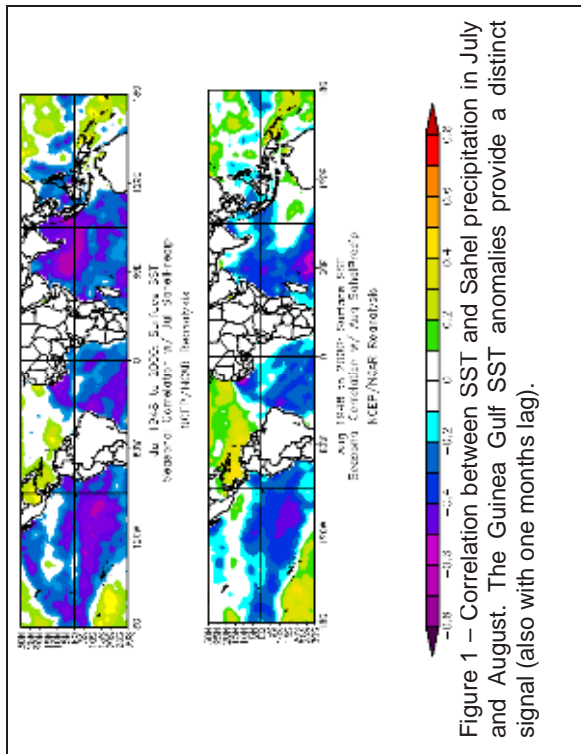
In Summer NCEP reanalysis shows three maxima of precipitation over Africa (Fig2c in Vizy and Cook, 2001). The precipitation occurs between the equator and 20 N, with the two major maxima located in the West and the East Africa region. The SSTs of the oceans have an influence on the pattern and the intensity of the precipitation. Palmer (1986) has investigated

---

\* *Corresponding author address:*

Marina Baldi CNR - IBIMET, Via Nizza 128, 00198  
- Roma, Italy. Phone: +39 06 4993-2812 ; FAX: +39 06  
4993-2730; Email: [m.baldi@ibimet.cnr.it](mailto:m.baldi@ibimet.cnr.it)

the role of the SSTAs of the tropical Atlantic, of the Indian Ocean and the Pacific using a GCM. He finds that the precipitation in West Africa is mainly influenced by the SSTAs of the Tropical Atlantic. The Northward extension of the African monsoon is limited by the Sahara through its high albedo, dry soil and beta effect (due to the large meridional extension of the desert), as shown by Chou and Neelin (2003).



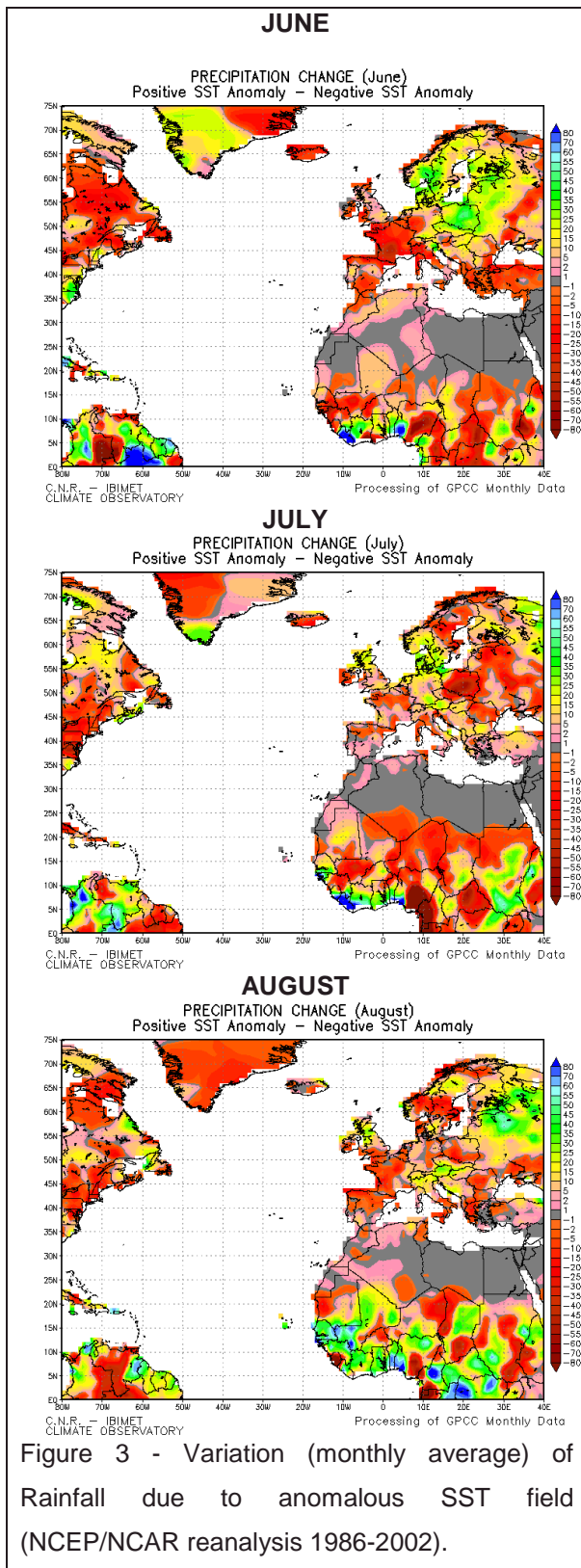


Figure 3 - Variation (monthly average) of Rainfall due to anomalous SST field (NCEP/NCAR reanalysis 1986-2002).

According to Rodwell and Hoskins (1996, 2001), the Indian monsoon induce subsidence over The East Sahara and the East Mediterranean sea through Rossby waves, probably reinforced by Charney (1975) mechanisms, i.e. feedback between the high albedo and the long wave radiation cooling due to the clear sky associated to the subsidence and the low humidity.

The influence the West African monsoon over the Sahara desert and on the West Mediterranean region is more controversial. Rodwell and Hoskins (1996) find only a marginal influence of the West African monsoon at the edge of the West Saharian-Mediterranean region. In addition, in this region there is a contribution to the subsidence due to the Svendrup effect, i.e. the Atlantic cyclone brings sinking air towards the equator, this effect is further enhanced by the blocking effect due to presence of the Atlas mountains.

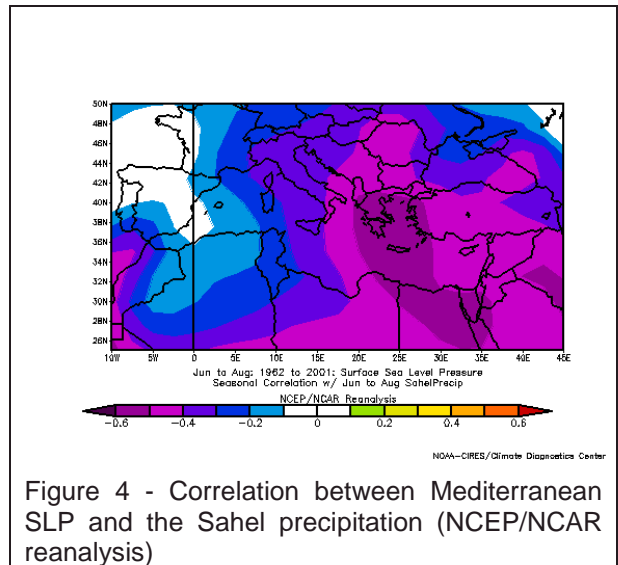


Figure 4 - Correlation between Mediterranean SLP and the Sahel precipitation (NCEP/NCAR reanalysis)

Vizy and Cook (2001, 2002) find that, in the presence of warm SST anomaly in the Gulf of Guinea, the precipitation increases near the coast and decreases over Congo farther inland. Northward and farther inland penetration of the

West monsoon is expected in the presence of cold SSTAs, even if the rainfall seems less sensitive to cold SSTAs.

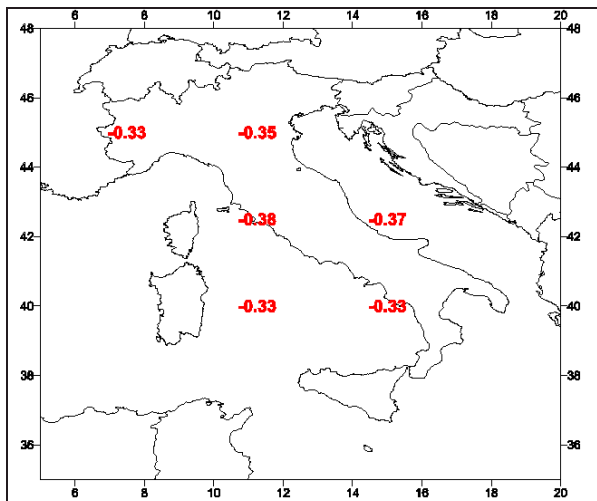


Figure 5 - 10% Significant Point correlation of CRU gridded rainfall with the Sahel Rainfall index for the period July and August

A climatological analysis suggests that the West Africa monsoon influence the central-western Mediterranean summer, and specifically the SLP (weakly), the temperature and the rainfall (see Figures 4, 5, 6a-6b). A southward shift of the monsoon is related to cooler and wetter conditions over the central and western Mediterranean sea in mid-late summer. While, when the monsoon influence moves further North, the summer is hot and dry over the Mediterranean sea.

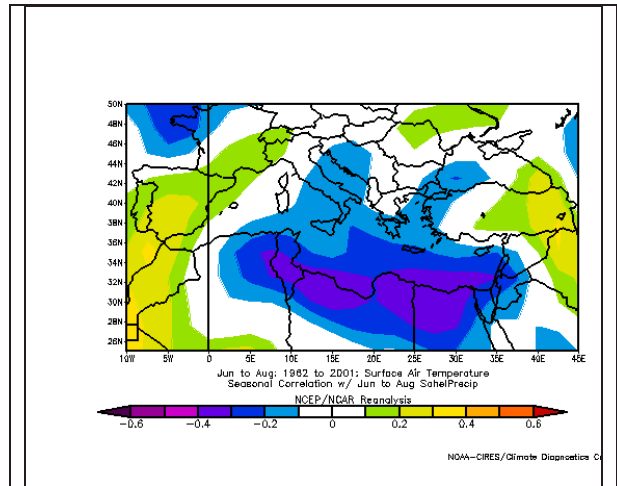


Figure 6a – Correlation of the Mediterranean surface air temperature at 850hPa and the Sahel precipitation (NCEP/NCAR reanalysis) for the summer period (JJA)

Numerical simulations were performed in order to investigate the impact of sea surface temperature anomalies (SSTAs) in the Gulf of Guinea on the Mediterranean climate, focusing, as a case study, on the summer 2002. During that summer, SSTAs in the Guinea Gulf were quite large and positive, while the central and western Mediterranean climate was anomalously wet and cool.

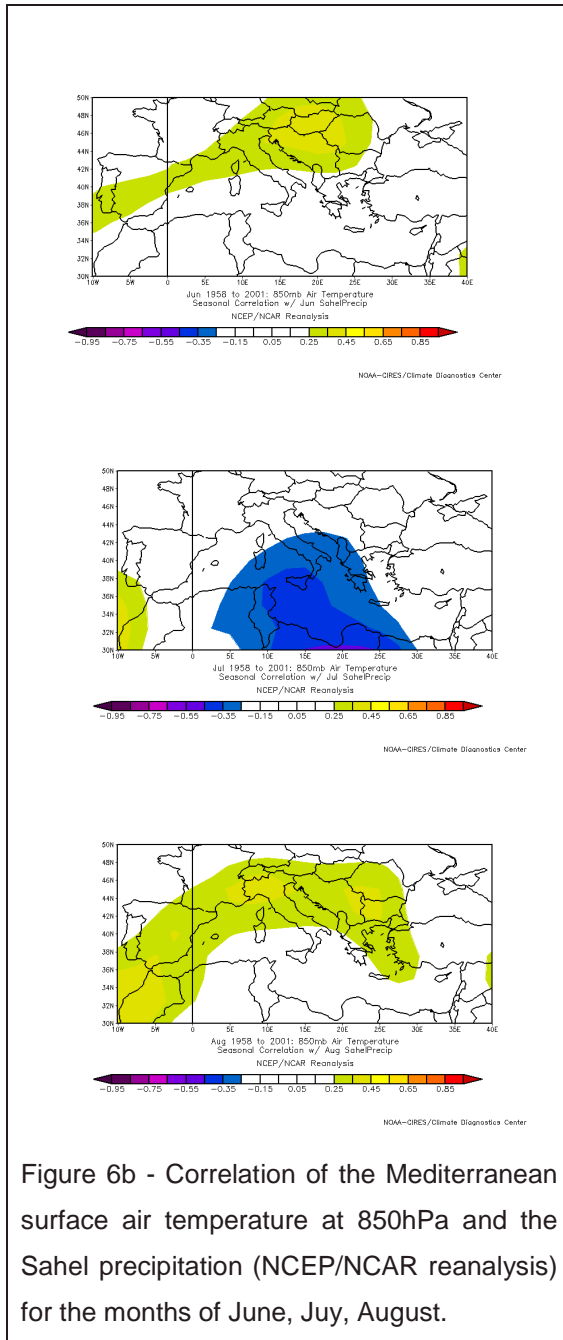


Figure 6b - Correlation of the Mediterranean surface air temperature at 850hPa and the Sahel precipitation (NCEP/NCAR reanalysis) for the months of June, July, August.

### 3. THE ANOMALOUS MEDITERRANEAN SUMMER 2002

In summer 2002 the Indian monsoon showed some “intriguing” aspects (Gadgil et al. 2003), and an anomalous climate characterized

the West Mediterranean and African region. June 2002 was warm as usual in West Africa, and warmer than average in western Europe, continuing the trend of the previous month. Very dry conditions persisted in parts of western and eastern Africa, and eastern Europe. Dry anomalies developed in western Europe, except for a band of an above-normal rainfall from the northern British Isles to Scandinavia. In the same month a band of below-normal rainfall extended from the Guinea Coast into parts of central and eastern Africa, including the region of the Great African Lakes, southern Sudan, and western Ethiopia. The SSTs off western Africa north of the equator stayed colder than average, while the warm anomaly, along the west coast of Southern Africa, which had developed during the previous months, decreased. The sub-tropical Atlantic, at about 30°N, was dominated by a warmer than average SST, with a moderate cold anomaly north and east.

July was unusually hot across southern and eastern Europe, with temperatures well above 40 C in some locations in southern Europe, with persistent deficit of rainfall across West Africa in the Sahel.

The SST off the West African coast north of the equator stayed colder than average, while the higher than average SSTs along the west coast of Southern Africa kept a decreasing trend.

August 2002 was warmer than average across northern and eastern Europe, while cooler than average temperatures were experienced along the Mediterranean coastal areas. Lack of rainfall persisted across West Africa in the Sahel, while heavy rains and

flooding affected most of central and eastern Europe.

The SST off of the West African coast north of the equator stayed cooler than average, while higher than average SSTs along the west coast of Southern Africa weakened. The midlatitudes SST colder than average persisted, as in July, in a broad west-east band extending from the eastern South Pacific into the southern South Atlantic basin.

Using NCEP/NCAR global reanalysis (Kalnay et al., 1996; Kistler et al., 2001), we analyzed in detail the events characterizing summer 2002 over Mediterranean, Europe and North Atlantic, in particular the anomalous SST and Sea Level Pressure (SLP) fields relatively to the mean climate patterns (Figure 1a, 1b).

In June, higher than normal SLP (1-3 hPa) were observed, when compared to the period 1961-1990, on the region going from subtropical Atlantic through the Mediterranean and eastern Europe, with very low pressures over the northern North Atlantic the British Isles and Scandinavia. The overall pattern changed in July, when a lower pressure developed from Iceland to central Mediterranean along a north-west to south-east axis, with anomalously high pressures in the south-west and north-east. In August, a band of anomalously high pressures developed from the mid-latitude North Atlantic up to the British Isles, Scandinavia and the north-eastern Europe, with lower pressures in central and southern Europe through central and western Mediterranean. The summer average SLP field was similar to the pattern observed in July.

The surface air temperature field over Mediterranean closely follows the sea level pressure patterns in summer (e.g. Maheras and Kutiel, 1999 ); in June 2002, temperatures in excess of 1-3°C respect to the period 1961-1990 developed over a large part of Mediterranean basin (Figure 1c), decreasing towards the mean climatological values in July, and below the average in August (specifically, over Italy the differences were of the order of +0.5 and - 1.25°C). The summer average surface temperature field exceeded the mean climatological values, as a result of the strong positive anomalies in June.

Focusing on the month of August, an anomalous precipitation pattern characterized the Mediterranean: it was extremely wet over central and southern Europe with a number of cases of severe flooding (Figure 2), whereas northern Europe experienced very dry conditions.

At the same time the African monsoon, forced by an atypically cold pattern of the SST in the Guinea Gulf (Figure 1a), north of the Equator and a smaller and less persistent warmer pattern south of the Equator, caused a drier than usual and below-normal rainfall condition across the Sahel region.

A blocking and persistent anticyclone over Europe was responsible of the splitting of the jetstream, the storm track split into two, with a north and a south branch.

Such a configuration was persistent for most of the summer, from July until early autumn, and developed into a weather pattern very similar to a fall configuration, with storms

affecting central and south Europe and penetrating deeply into the Mediterranean.

#### 4. MODEL DESCRIPTION AND DESIGN OF THE NUMERICAL EXPERIMENT

The atmospheric numerical model adopted is the Regional Atmospheric Modeling System (RAMS) developed at the Colorado State University and at MRC/\*ASTER, now maintained and distributed by ATMET (<http://www.atmet.com>). RAMS is a general-purpose, coupled atmosphere-land surface simulation model that includes the equations of motion, heat, moisture, and continuity in a terrain-following coordinate system. It is capable of modeling in details a wide range of atmospheric phenomena providing important research insights into the basic dynamics of interrelated weather, climate, and Earth system processes. RAMS has been widely used to simulate relatively short-term atmospheric processes, and the interactions between atmospheric process and forcing at the surface (Pielke et al., 1992).

In the present study, RAMS is configured at 60 km horizontal resolution, over a domain extending south to the Guinea Gulf and north to Scandinavia and covering most of Europe, equatorial and northern Africa and equatorial and northern Atlantic, and Mediterranean (Figure 7). The simulations have been initialized on May 15<sup>th</sup>, 2002 and run until August 31<sup>st</sup>, 2002, with initial and boundary conditions provided by

the global atmospheric and surface NCEP/NCAR reanalyses at 2.5° Lat-Lon horizontal resolution (E. Kalnay et al., 1996; Kistler et al., 2001). The impacts of the West Africa summer monsoon over the Mediterranean region has been analyzed by selectively modifying the major forcing of that tropical circulation, i.e. the Gulf of Guinea sea surface temperature.

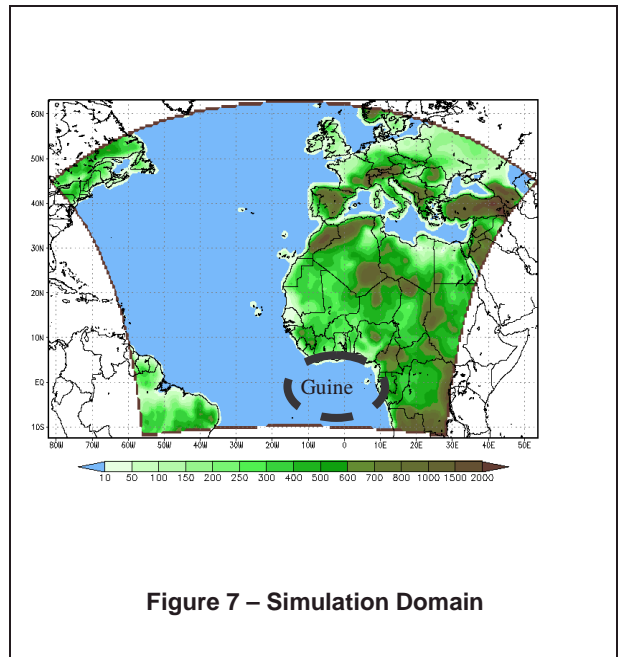


Figure 7 – Simulation Domain

In order to assess the model's ability to reproduce both the detailed monsoon precipitation regime and the monthly Mediterranean and West Africa rainfall patterns, results have been compared both with the monthly mean precipitation fields, provided by the Global Precipitation Climatology Centre (GPCC: Schneider, 1993 ; Xie et al., 1996), over a regular grid covering the same area, and built on the basis of rain gauges observations, at a resolution of 1° Lat-Lon, and with the 5-day cumulated precipitation field provided by the Global Precipitation Climatology Project (GPCP:

Xie et al., 2003 ), over the three monsoonal areas in West Africa at a resolution of 2.5° Lat-Lon, created integrating rain gauges and satellite observations.

A “control” simulation (hereafter “cR” simulation) was initialized with the observed SST, while a “perturbed” simulation (hereafter “pR” simulation) consisted in a similar simulation as in the cR, where the original SST field has been perturbed by introducing a cooler SST dipole in the Guinea Gulf, with peaks of -2°C and intensity decreasing as the square of distance up to a fixed radius (Figure 8). The control and perturbed simulations have been inter-compared in terms of monthly sea level pressure and geopotential height fields, precipitation patterns and storm track pattern and intensity, as shown in the next section.

## 5. RESULTS

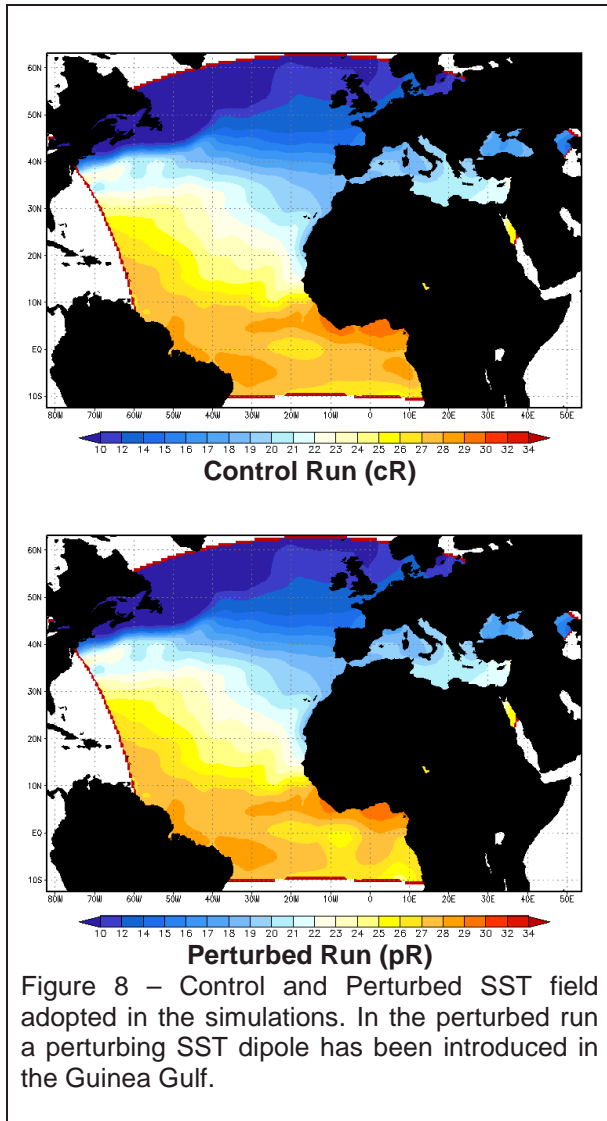
The results from the cR simulation have been compared with the monthly GPCC gridded precipitation field over land for the month of June, July and August 2002 (see Figure 9a, and 9b for August 2002).

In June although the simulated inter-tropical convective precipitation pattern is qualitatively similar to the observations, however the cR simulation overestimates the precipitation around 5°N, east of 10°E, and extends too far north, 15°N and it is most probably due to an excess of the initial soil moisture in the region north of the Sahel and Sahara (the soil moisture is initialized as homogenous over the entire domain). The simulated precipitation is underestimated over most of continental Europe

and, particularly, over the Iberian Peninsula, the northern Mediterranean coast and the Balkans.

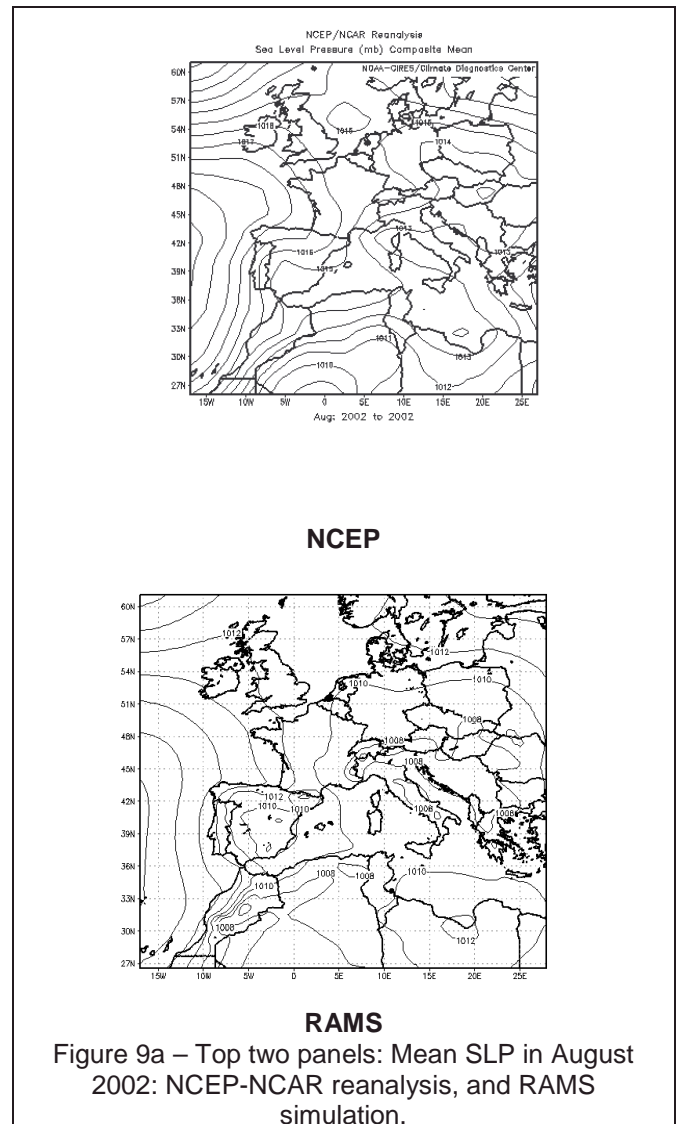
In July, the inter-tropical precipitation over Africa is well simulated, as well as its northernmost extent; with an underestimation near the border between Nigeria and Cameroon (about 10°E, 5°N) and an overestimation north-east of that area (around 20°E, 8°N). The precipitation patterns are well reproduced by the model over southern Europe, although locally they are underestimated in places: for example the total rainfall simulated over central Europe and the Alps is about half of the observed precipitation.

In August (Figure 9a) the simulated precipitation in the tropics is in good agreement with the observations, with an over-estimation around 20°E, 8°N. The simulated rainfall fails, to some extent, over central and the western Mediterranean and western Europe, where very little (or no) precipitation is produced, while there is an observed average of 80 mm over land. A similar absolute magnitude is found in central Europe and British Isles.



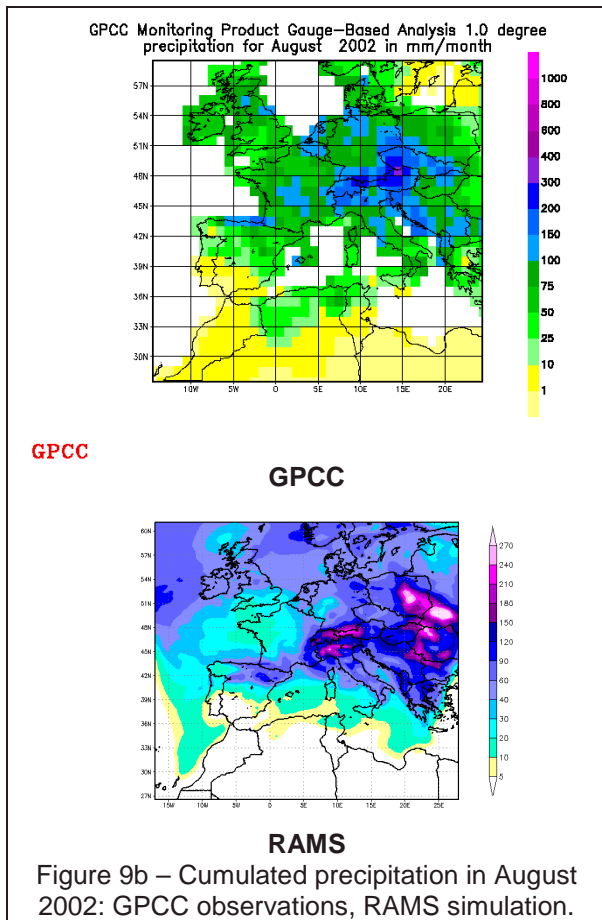
The large simulation error, found over land in the Mediterranean and Europe, could be due to the joint effects of the coarse spatial horizontal resolution (60 km) and the “modified-Kuo” cumulus convection parameterization scheme used in RAMS (Molinari, 1995), which suffers from several deficiencies. In this respect, an extensive review of currently used cumulus schemes can be found in Pielke (2002), while Meneguzzo et al. (2003) investigated the impact of horizontal spatial resolution on quantitative precipitation forecasts, down to a less than 2 km

of grid spacing, showing that the use of coarse resolution grids (e.g. 16 km) with the modified-Kuo cumulus convection parameterization scheme is not able to produce satisfactory precipitation fields, which were produced over finer resolution grids where convection was explicit.



Castro et al. (2001) have shown the enhanced efficiency of the Kain-Fritsch (KF) cumulus parameterization scheme respect to the modified Kuo scheme. The KF scheme is now

implemented in RAMS and it will be used for future numerical investigations.



The cumulated precipitation simulated by the cR have been compared with the GPCP pentad precipitation analyses (Xie et al., 2003) over three test areas: Guinea Coast (GC), Southern Sahel (SS) and Northern Sahel (NS) (see Figure 10, top panel), representative of the West Africa monsoon development and phases. In this respect an analysis has been performed in order to verify whether RAMS is able to capture the typical abrupt northward shift of Inter-Tropical Convergence Zone (ITCZ) and the associated rainfall well depicted by the sudden increase of the daily rainfall at 15°N, averaged

over 10°W-10°E, as in Sultan and Janicot (2000). This abrupt transition of the ITCZ is in turn associated to the relative decrease of rainfall over the Guinea Coast and the increase over the Sahel. The mean date for this abrupt shift over the period 1968-1990 is 24 June with a standard deviation of 8 days.

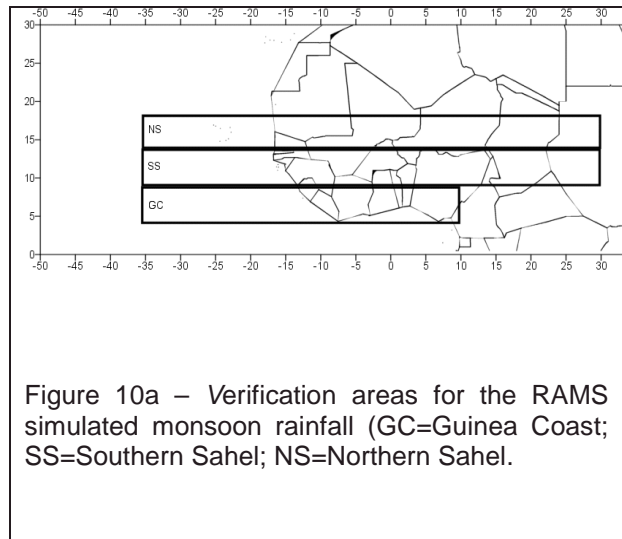


Figure 10 shows the comparison between the pentad rainfall estimated by GPCP and by the cR simulation, averaged over the three areas GC, SS, NS, from June to August, 2002. The GPCP estimates show an abrupt increase of rainfall over the NS area (i.e. around 15°N) in the first pentad of July 2002, quite consistent with the literature (Sultan and Janicot, 2000; Sultan and Janicot, 2003), which is partly reproduced by RAMS, partly masked by the over-estimation during June. A similar behavior appears over the SS area, where the shift is less pronounced but is quite well reproduced by RAMS. During the same period, a relative and temporary decrease of rainfall over the GC area is shown by the GPCP data, and RAMS

reproduces, with a delay of about 10 days, a similar sudden decrease. Later in the summer, after July 15, the cR simulation under-estimates by about 50-60% the rainfall reconstructed by GPCP over the GC and SS areas, while the simulated rainfall agrees quite well with the observations over the NS area till August 10, after that a relevant under-estimation appears.

The relative differences in the results between cR and pR simulations are shown in Figure 11a, 11b, 11c. Figure 11b shows the monthly mean fields of sea level pressure (SLP) produced by the cR and the pR simulations. In June, the only appreciable impact of the perturbation applied to the SST over the Guinea Gulf consists in the broadening of the thermal low over the Sahara desert centered around  $2^{\circ}\text{E}$ ,  $23^{\circ}\text{N}$ , which slightly increases the meridional pressure gradient between the Guinea Coast and the northern Sahel; in July and August, no relevant effects are present.

The impact of the perturbations applied to the SST over the Guinea Gulf appears stronger and more evident in the structure of the 500 hPa geopotential field (see Figure 11c). In June, the intensity of the ridge over the African sub-tropics is slightly reduced, while a moderate trough appears in the eastern North Atlantic around  $35^{\circ}\text{N}$ , the geopotential height decreases also over the southern Mediterranean and increases from the northern Mediterranean coast to the north-western Europe, probably as a dynamical and thermal response to the trough over the eastern North Atlantic. In July, a very relevant impact of the perturbation is shown as the offset of the trough produced by the cR simulation over Italy and northern Balkans, and

the increase of geopotential heights over central and western Mediterranean and most of Europe south of  $50^{\circ}\text{N}$ . Since no other relevant difference is shown west of this area (i.e. over North Atlantic), the mechanisms acting to produce this impact could be linked to a transformation or shift of the meridional overturning circulation, i.e. the regional Hadley cell over northern Africa in turn connected to the monsoon circulation (see Dima and Wallace, 2003, for a detailed discussion on the regional Hadley circulations).

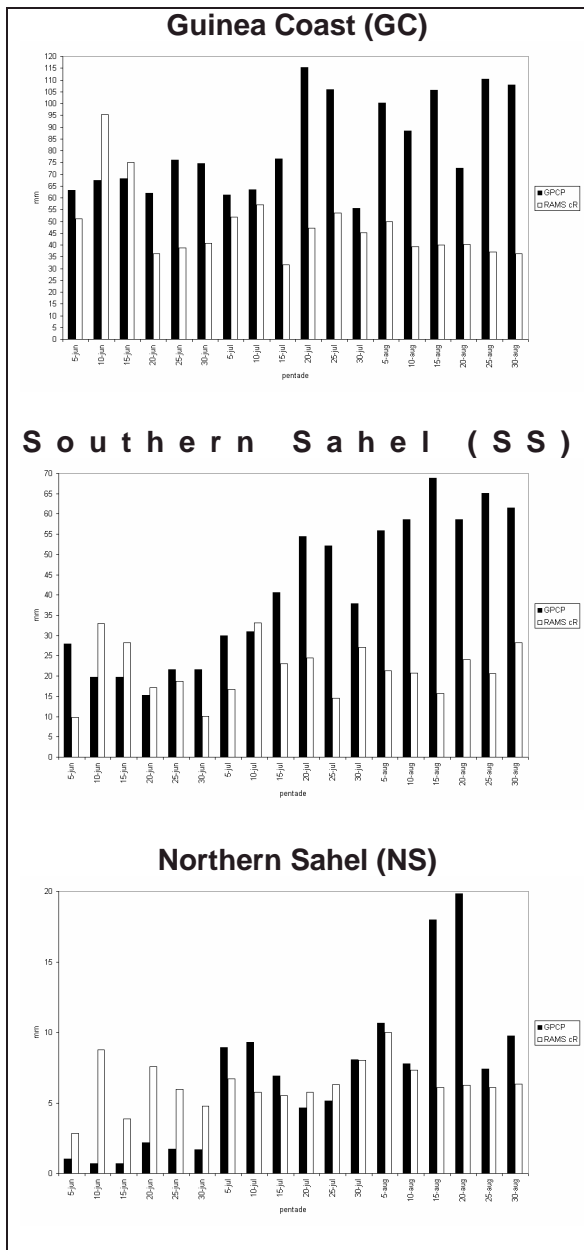


Figure 10b – Pentad cumulated rainfall. Comparison between GPCP estimate and RAMS cR simulation over the areas GC, SS and NS (see text for details).

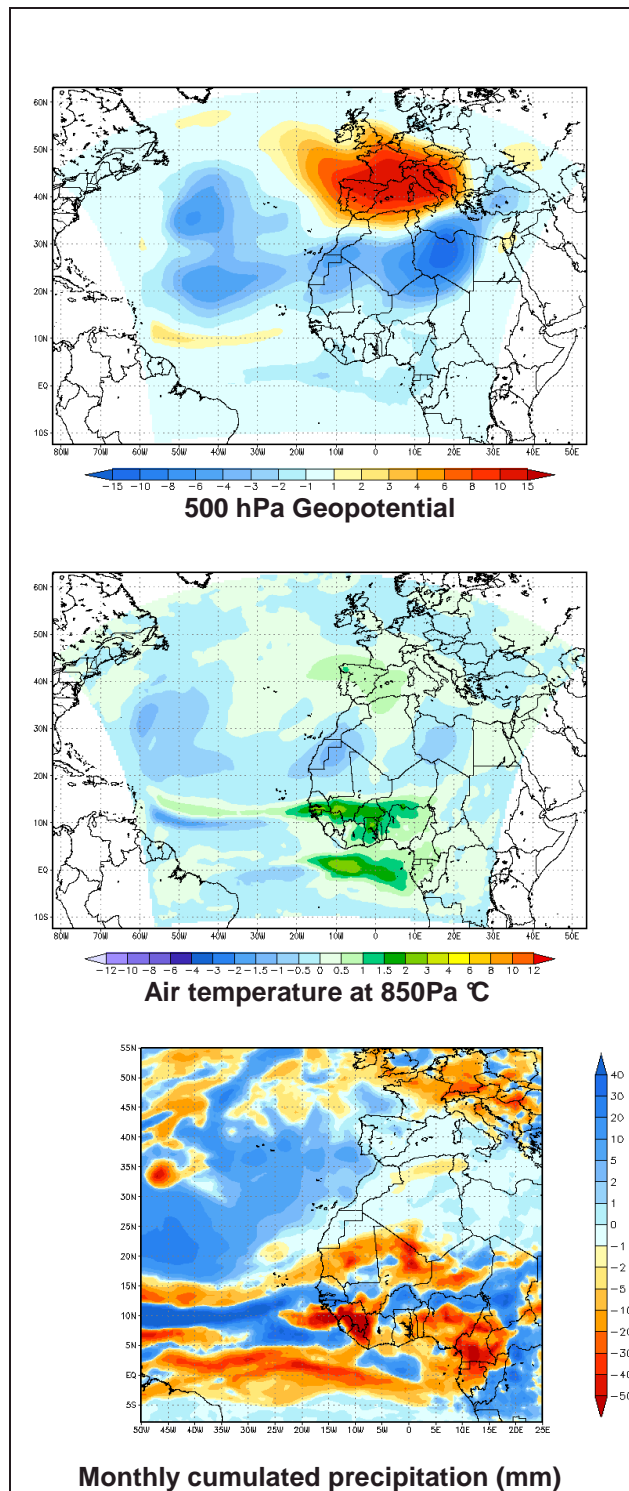


Figure 11a – Difference between Perturbed and Control Run: geopotential height, air temperature, and cumulated precipitation in August 2002.

Similar impacts are revealed in August, when the perturbed simulation produces a ridge extending from the subtropical northern Africa to the Alps, slightly decreasing the peak geopotential heights over the Sahara and increasing it over central and western Mediterranean.

been analyzed along the 0 meridian from 5°S to 24°N, as in Vizy and Cook (2002). Figure 12 shows the streamlines, meridional and vertical wind component, (this latest multiplied by a 1,000 factor), as produced by the cR and by the pR simulation.

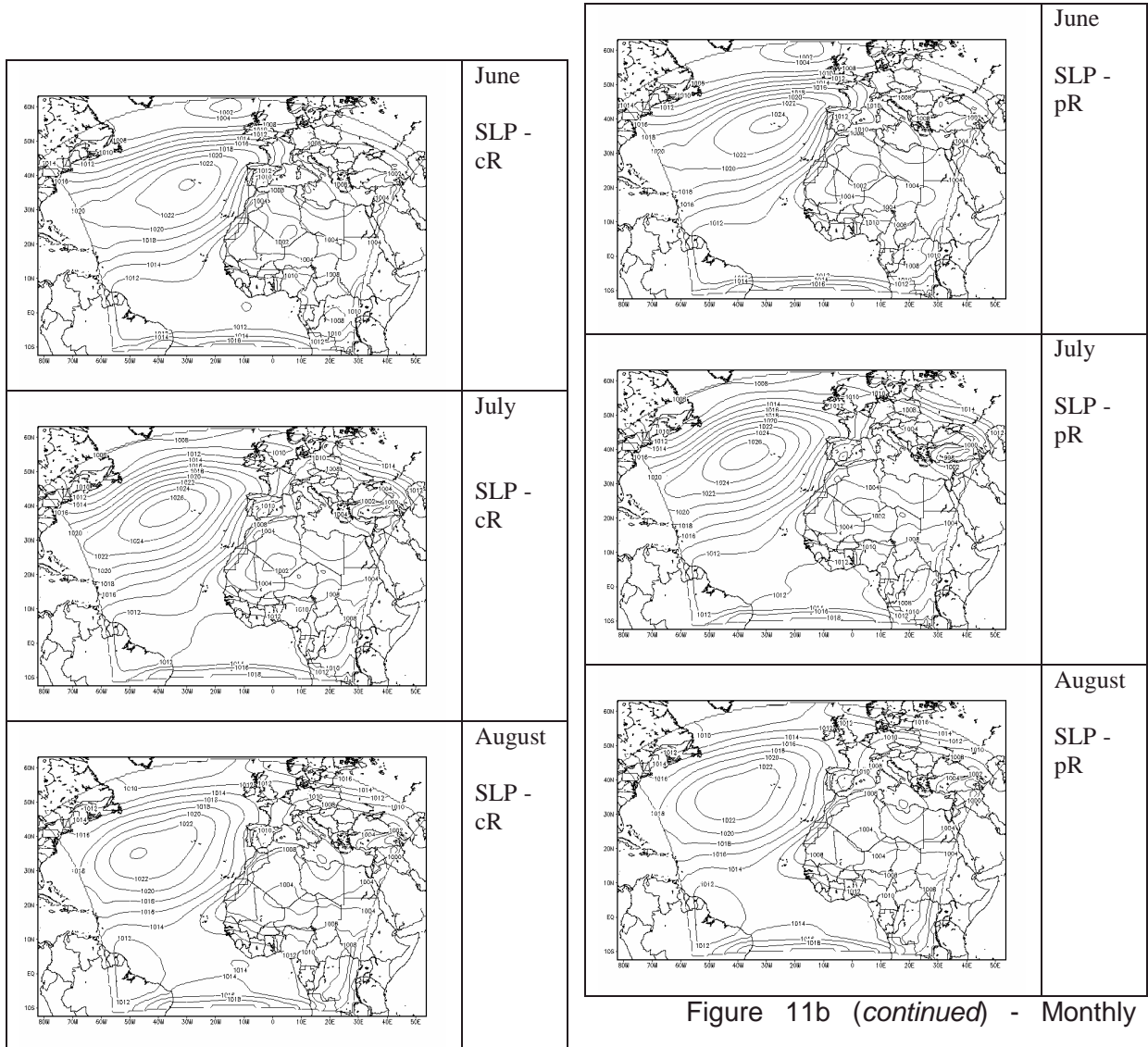


Figure 11b - Monthly mean of the SLP (hPa), June-July-August 2002: control simulation.

Figure 11b (continued) - Monthly mean of the SLP (hPa), June-July-August 2002: perturbed simulation.

In order to investigate the role of the Meridional Circulation, the meridional vertical cross section of some physical parameters have

In June, the Hadley cell, zonally averaged through the domain, with its rising branch around 5°N is slightly shifted northward in

the pR. Regionally, the Hadley cell is shifted about 3° northward to 16°N, because of the well developed monsoonal circulation, with a more vigorous convergence in the south, and subsidence north of 22°N. In Figure 13, where the vertical cross section is extended northward to 55°N, there is an evident northward shift of the influence of African Continent on the atmospheric flow. In June, in the upper troposphere, at 300hPa (ca), there is a vortex at 38°N, with an enhanced subsidence at 37°N and upwelling at 40°N and northward flux toward higher latitudes. An enhanced subsidence is also produced by the pR in the mid-low troposphere at 37°N.

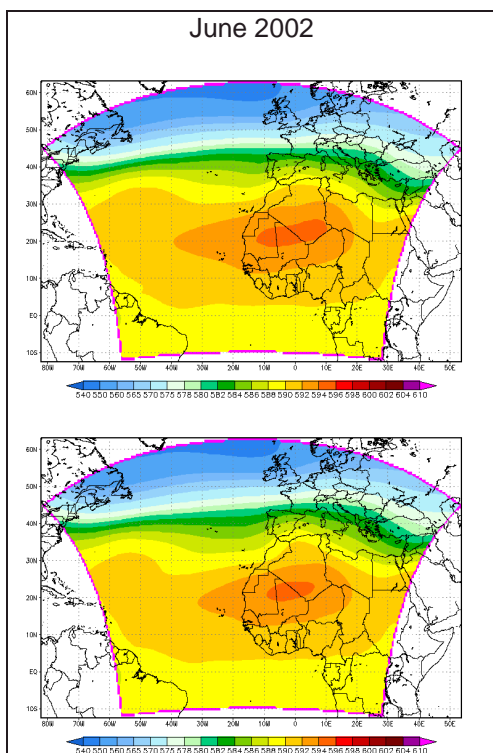


Figure 11c - Difference of the monthly mean fields of Geopotential height at 500 hPa produced by the perturbed (pR) and control (cR) RAMS simulations (top and bottom panel)

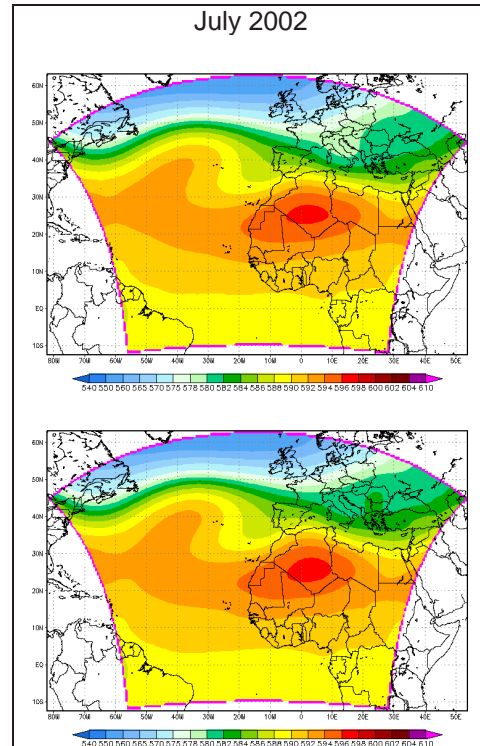


Figure 11c - Continued for July

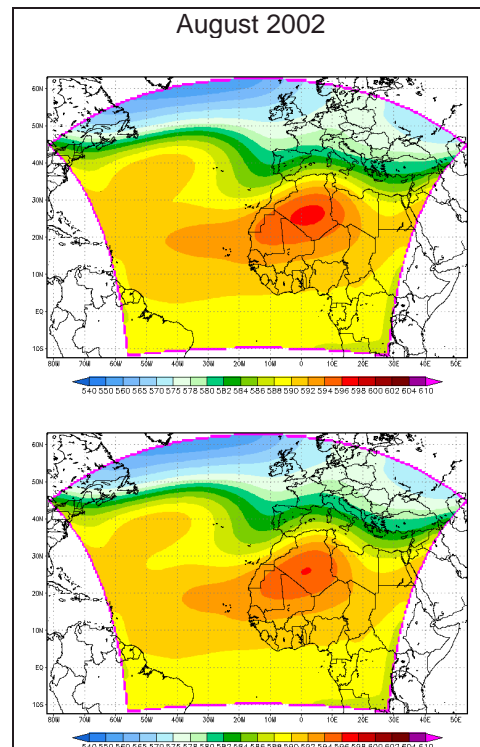


Figure 11c - Continued for August

In Figure 14, a vertical cross section as in Figure 13 shows the difference of the potential temperature field produced by the pR and the cR simulations, while Figure 15 shows the difference of the equivalent potential temperature field produced by the pR and the cR simulations. The most major feature, in June, is represented by the strong (about 0.5K) cooling around 25°N up to an altitude of about 650 hPa, and a general cooling of similar magnitude in the layer between 500 hPa and 250 hPa, spanning the latitudes from 15°N to 45°N, and a larger warming (with a peak of 3K) above 220 hPa, from 10°N to 35°N. A broad area with significant warming is produced in the lower troposphere from 35°N to 47°N, extending from the surface up to about 600 hPa, with an intensity of about 0.5K.

A little more can be added on the precipitations over the area, and in particular on the effect due to a modified SST field. Figure 16 shows the differences the five-days cumulated rainfall between cR and pR over three areas: GC, SS, NS. The two simulations produce a very similar pentadal pattern over the three areas, and both are able to catch the summer monsoonal regime variability, although the pR precipitation is almost always less than the cR precipitation, until mid-July. Later on the differences reduce to a minimum in late summer; only over SS the pR precipitation is higher than the cR, in the period July 20<sup>th</sup> to August 20<sup>th</sup>. The fact that cR precipitation is greater than the pR precipitation almost always even over NS (except in the second half of July) is probably due to the fact that the increased evaporation from the warmer sea surface in cR is more effective than the reduced land-sea temperature

contrast in enhancing precipitation far north (Vizy and Cook, 2002), thus emphasizing the role that SST have in the triggering of the monsoon.

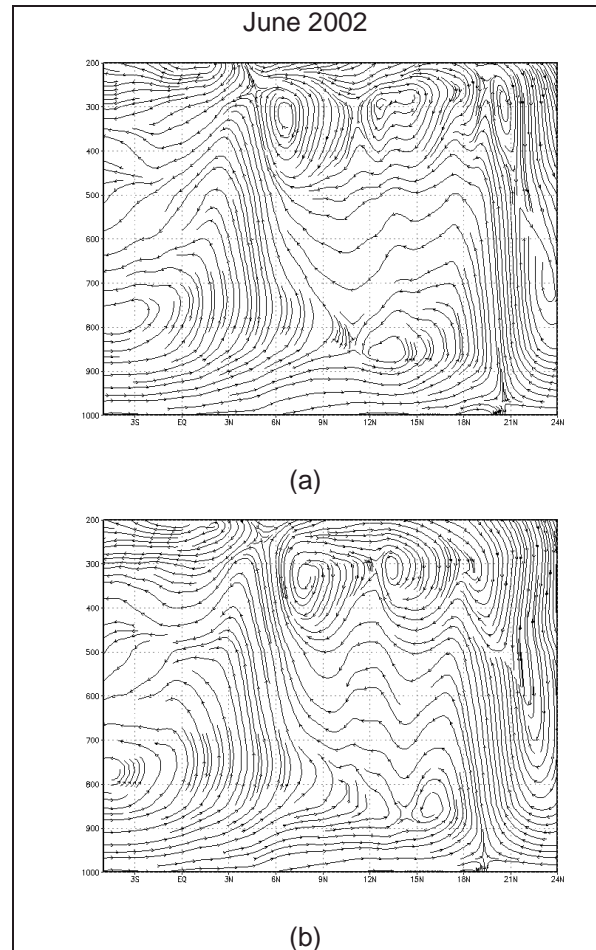


Figure 12 - Monthly mean streamlines in June (a, b) and August (c, d) given by the composition of the meridional and vertical components of the wind (the vertical component being multiplied by 1,000) along a vertical section at 0°W longitude, from 5°S to 24°N, produced by the control (cR: a, b) and the perturbed (pR: c, d) RAMS simulations

## 6. CONCLUSION

A connection between the summer rainfall patterns over the Mediterranean and the African monsoon index, i.e. the Sahel precipitation has been shown both by the NCEP-NCAR reanalysis and by model simulations. Moreover, a link between the SST and SSTA in the Gulf of Guinea, and both the Sahel precipitation and the Mediterranean climate have been shown, more prominent during the month of August.

the moisture flux over the entire region, giving rise to anomalous amounts of available moisture which produces, in turn, anomalous precipitation patterns in particular over Mediterranean.

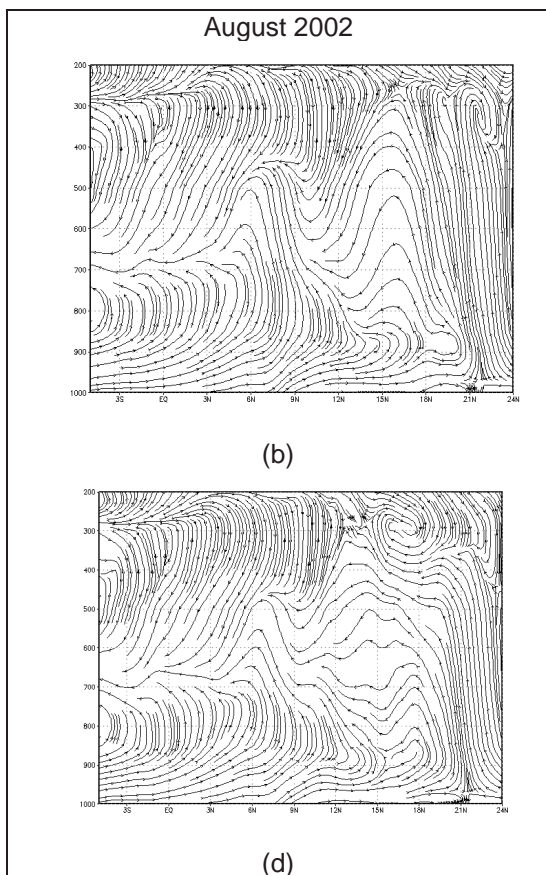


Figure 12 – Continued

Sensitivity runs show how the SST anomalies can produce quantitatively significant anomalies in the sea level pressure patterns over North Sahel (positive) and Mediterranean (negative), in the 500hPa geopotential, and in

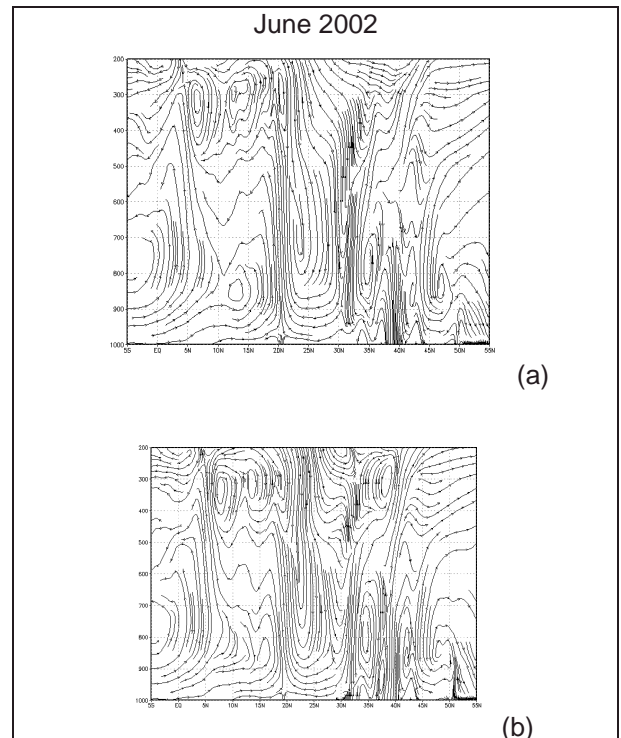


Figure 13 - Monthly mean streamlines in June (a, b) and August (c, d) given by the composition of the meridional and vertical components of the wind (the vertical component being multiplied by 1,000) along a vertical section at 0°W longitude, from 5°S to 55°N, produced by the control (cR: a, b) and the perturbed (pR: c, d) RAMS simulations

The influence of the SSTAs of the eastern tropical Atlantic is evident on the 500 hPa geopotential over the Mediterranean. Whereby, cooler SSTs over the Gulf of Guinea

produce a significant increase over western Mediterranean and a smaller decrease over southern-eastern Mediterranean, extending through northern Sahara and subtropical north Atlantic.

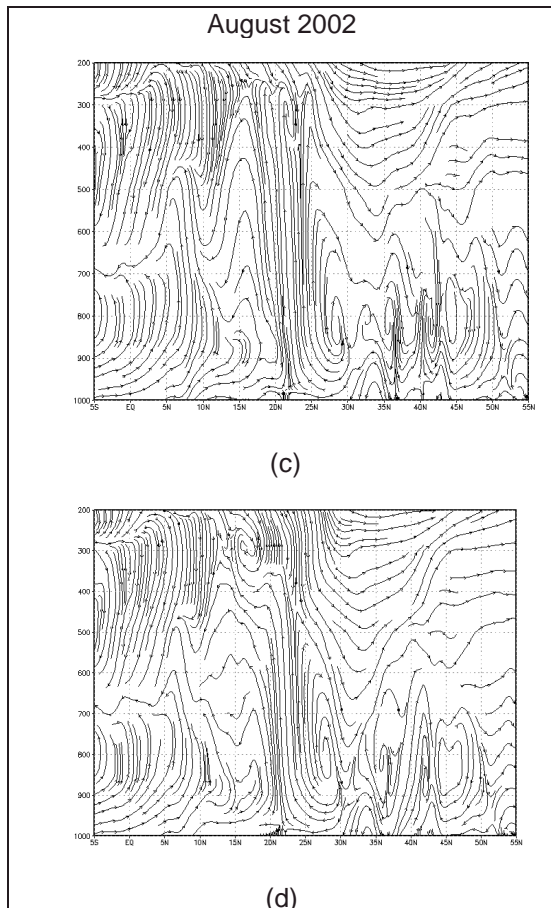


Figure 13 – *Continued*

The different SSTs make a significant difference on the amount of precipitation over central and northern Italy, France, central Europe and Balkans. Cooler SSTAs are bounded to a substantial decrease of precipitation, which is in agreement with a higher mid-tropospheric geopotential.

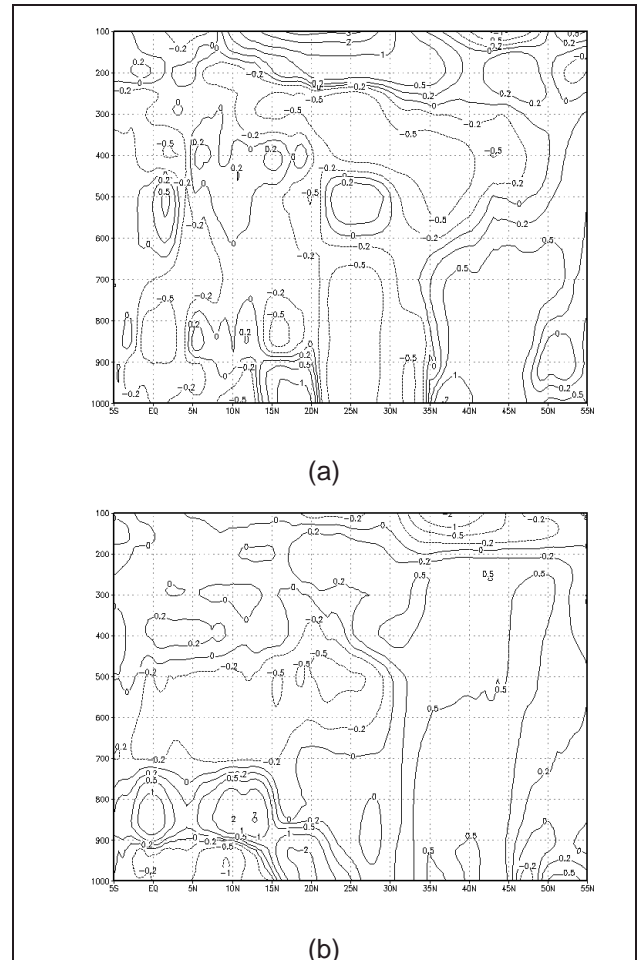


Figure 14 - Difference of the monthly mean potential temperature June (a) and August (b) along a vertical section at 0°W, from 5°S to 55°N, produced by the perturbed (pR) and control (cR) RAMS simulations

A further perturbation, which affects the north Atlantic storm track, is given by the low level moisture advection over the area.

Sizable changes in the physical parameters are observed over tropical and subtropical north Africa, which are qualitatively well reproduced by the simulations. In particular, a clear modification of the abrupt transition of the ITCZ and the associated monsoon system over Sahel, which usually occurs in the last week of June, (Sultan and Janicot 2000; 2003 when the

seasonal rain over the Gulf of Guinea almost stops and precipitations over Sahel Region begin, is well represented by the numerical experiment.

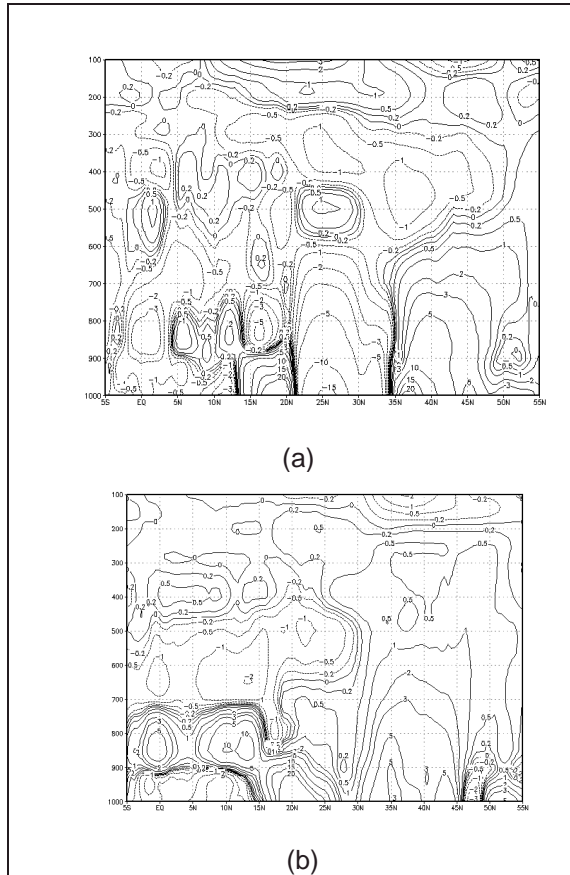


Figure 15 - Difference between the perturbed (pR) and control (cR) RAMS simulations of the monthly mean equivalent potential temperature June (a) and August (b) along a vertical section at 0°W, from 5°S to 55°N.

The performance of the cR simulation has been evaluated comparing numerical results with the five-day global gridded cumulated precipitation estimated by the GPCP, over three areas: Guinea Coast (GC), Southern Sahel (SS) and Northern Sahel (NS).

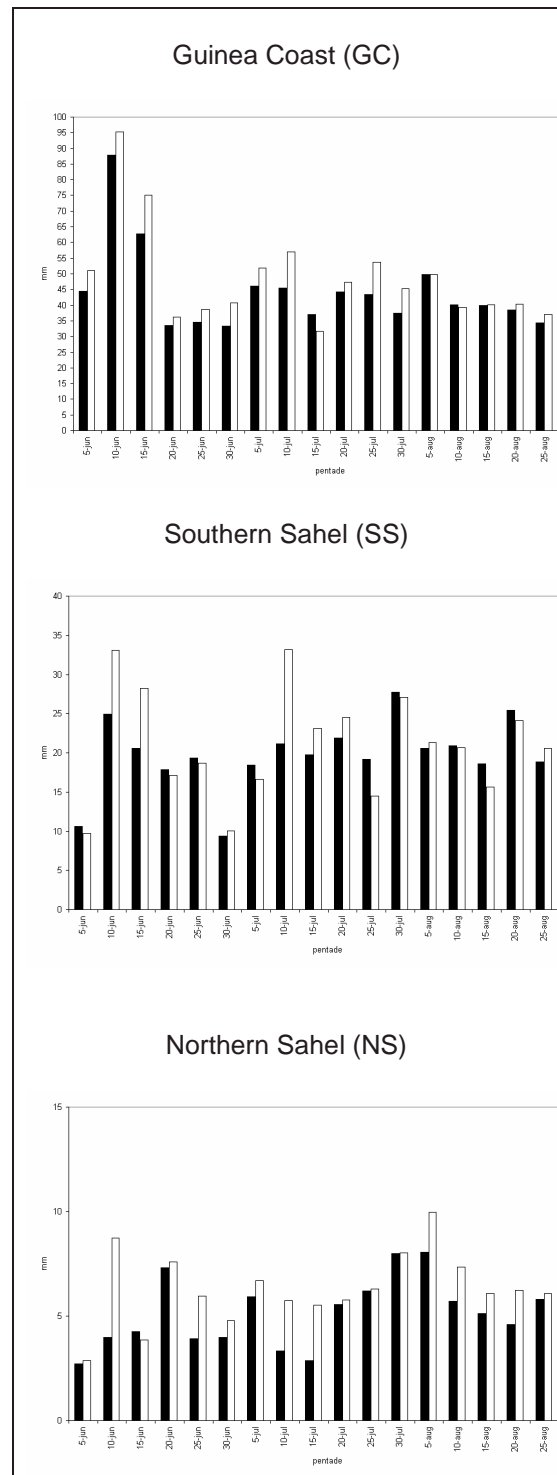


Figure 16 - Comparison of the five-days cumulated rainfall produced by the control (cR) and perturbed (pR) RAMS simulations over the areas GC, SS and NS.

A strong correlation is found of the precipitation time series over the GC area (correlation coefficient of 0.96), which decreases further north with a correlation coefficient of 0.8 over the SS, and 0.7 over the NS area.

In addition, a shift of the Atlantic storm track towards North Europe, when the African monsoon is more vigorous, is evident from the simulations, although the simulated perturbations of the storm track are less intense than the perturbations shown by the NCEP/NCAR reanalysis.

In order to assess the effectiveness of modified SST on the monsoonal regime, the pR and cR simulations results have been compared. In terms of precipitations, the pR is almost always less than the cR precipitation, especially till mid-July, after that time, the differences reduce to a minimum in late summer; only over SS the pR precipitation is higher than the cR, in the period July 20<sup>th</sup> to August 20<sup>th</sup>. The fact that cR precipitation is greater than the pR precipitation almost always even over NS (except in the second half of July) is quite surprising, although Vizu and Cook (2002) suggest that the increased evaporation from the warmer sea surface in cR is probably more effective than the reduced land-sea temperature contrast to enhance precipitation far north.

This last hypothesis, and the preliminary results shown here need further investigation of the mechanism through which the SSTA in the Gulf of Guinea affect the summer climate of the Mediterranean Region, and of the feedback that the SST and SSTAs in the Mediterranean Basin have over the Sahel precipitation and in particular on the variability of the so-called fast

transition period. A climate version of RAMS will be used to perform long term simulations (seasonal and yearly) over the same Mediterranean-North African Region in order to study long term variability of the Mediterranean climate.

### **Acknowledgments**

The Authors thank the Climate Diagnostic Center (NOAA, Boulder, CO) for providing the NCEP/NCAR Reanalysis dataset and the Project "Improvement of the management of water resources and crop yield in hazardous areas with regard to drought and desertification" of the Italian Presidency of the Council of Ministries.

M. Baldi and G.A. Dalu acknowledge the National Science Foundation under Grant No. ATM-9910857, and the Italian CNR Short-Term Mobility Program.

### **References**

- Castro, C.L., R.A. Pielke, G.E. Liston, 2001: Simulation of the North American monsoon in different Pacific SST regimes using RAMS, paper presented at the 26<sup>th</sup> Annual Climate Diagnostics and Prediction Workshop, La Jolla (CA), October 22-26, 2001.
- Chou, C., and J. D. Neelin, 2003: Mechanisms limiting the northward extent of the northern summer monsoon over North America, Asia, and Africa, *J. of Climate* **16**, 406-425.
- Dima, I.M., J.M. Wallace, 2003: On the seasonality of the Hadley cell. *J. of Atmos. Sc.*, **60**, 1522-1527.

- Gadgil S., J. S., R. S. Nanjundiah, K. K. Kumar, A. A. Munot, R. K. Kolli, 2003: On Forecasting the Indian Summer Monsoon : the Intriguing Season of 2002. (Submitted to Current Science)
- Kalnay E., M. Kanamitsu, R. Kistler, W. Collins, D. Deaven, L. Gandin, M. Iredell, S. Saha, G. White, J. Woollen, Y. Zhu, N. Chelliah, W. Ebisuzaki, W. Higgins, J. Janowiak, K.C. Mo, C. Ropelewski, J. Wang, A. Leetmaa, R. Reynolds, R. Jenne, and D. Joseph, 1996: The NCEP/NCAR 40-Year Reanalysis Project. *Bull Am Met Soc*, **77**, 437-471.
- Kistler R., E. Kalnay, W. Collins, S. Saha, G. White, J. Woollen, M. Chelliah, W. Ebisuzaki, M. Kanamitsu, V. Kousky, H. van den Dool, R. Jenne, and M. Fiorino, 2001: The NCEP–NCAR 50-Year Reanalysis: Monthly Means CD-ROM and Documentation. *Bull Am Met Soc*, **82**, 247-268
- Maheras P., H. Kutiel, 1999: Spatial and temporal variations in the temperature regime in the Mediterranean and their relationship with circulation during the last century. *Int. J. Climatol.*, **19**, 745-764.
- Meneguzzo, F., M. Pasqui, G. Menduni, G. Messeri, B. Gozzini, D. Grifoni, M. Rossi, G. Maracchi, 2003: Sensitivity of meteorological high-resolution numerical simulations of the biggest floods occurred over the Arno river basin, Italy, in the 20th century. Accepted for publication in: *Journal of Hydrology*.
- Molinari, J., 1985: A general form of Kuo's cumulus parameterisation. *Monthly Weather Review* **113**, 1411-1416
- Pielke, R. A., Cotton, W. R., Walko, R. L., Tremback, C. J., Lyons, W. A., Grasso, L. D., Nicholls, M. E., Moran, M. D., Wesley, D. A., Lee, T. J., Copeland, J. H., 1992: A comprehensive meteorological modeling system - RAMS. *Meteorol. Atmos. Phys.*, **49**, 69-91.
- Pielke, R.A., 2002: *Mesoscale Meteorological Modeling*. 2nd Edition, Academic Press, New York, N.Y., 612 pp.
- Rodwell, M.J. and Hoskins, B.J., 1996: Monsoons and the dynamics of deserts. *Q. J. R. Meteorol. Soc.*, **122**, 1385-1404.
- Rowell, D.P., 2003: The impact of Mediterranean SSTs on the Sahelian rainfall season, *J. of Climate* **16**, 849-862.
- Schneider, U., 1993: The GPCC quality-control system for gauge measured precipitation data. GEWEX Workshop on Analysis Methods of Precipitation on Global Scale, Rep. WCRP-81, WMP/TD-588, Koblenz, Germany, WMO, A5–A9
- Sultan B., S. Janicot, 2000: Abrupt shift of the ITCZ over West Africa, *Geophys. Res. Letter*, vol. 27, 20, 3353-3356
- Sultan B., S. Janicot, 2003: The West African monsoon dynamics. Part II the pre-onset and the onset of the summer monsoon, *Journal of Climate* (in press)
- Vizy, E. K., and K. H. Cook, 2001: Mechanisms by which Gulf of Guinea and Eastern North Atlantic sea surface temperature anomalies can influence

African rainfall., J. of Climate **14**, 795-821

Vizy, E. K., and K. H. Cook, 2002: Development and application of a mesoscale climate model for the tropics: Influence of sea surface temperature anomalies on the West African monsoon, J. Geophys. Res.- Atmos., **107(D3)**, 10.1029/2001JD000686

Xie, P., and P. A. Arkin, 1996: Analyses of global monthly precipitation using gauge observations, satellite estimates, and numerical model predictions. J. Climate, **9**, 840–858

Xie, P., Janowiak, J. E., Arkin, P. A., Adler, R., Gruber, A., Ferraro, R., Huffman, G. J., and S. Curtis, 2003: GPCP pentad precipitation analyses: an experimental dataset based on gauge observations and satellite estimates. J. Climate, **16**, 2197-2214